International Research Journal of Engineering and Technology (IRJET) e-ISSN: 2395-0056
Volume: 05 Issue: 05 | May-2018 www.irjet.net p-ISSN: 2395-0072

VISUALIZATION OF HOT WIRE GAS TUNGSTEN ARC WELDING PROCESS

Dinesh. K[1], Anandavel. B[2], Devakumaran. K[3]

[1] *Dept. of Metallurgical Engineering, Government College of Engineering, Salem, Tamil Nadu, India.*
[2] *Asso. Professor, Dept. of Metallurgical Engineering, Government College of Engineering, Salem, Tamil Nadu, India.*
[3] *Deputy Manager, Welding Research Institute, BHEL, Tiruchirappalli, Tamil Nadu, India.*

Abstract – *The hot wire-gas tungsten arc welding process is where the filler wire is resistance heated before feeding into arc for some special performances. The beads are deposited on the surface of alloy 617 tube with the help of hot wire gas tungsten arc welding process. Hot wire gas tungsten arc welding (HW-GTAW) process is the one where the filler wire is preheated close to its melting point before it is fed in to the arc. The effect of HW-GTAW parameters such as welding current and hot wire current during the deposition of beads on the alloy 617 tube was evaluated in terms of cooling rate, heat input and weld bead characterization such as macrostructure, microstructure, micro hardness survey and SEM analysis. The influence of welding current along with the hot wire current influences the deposition rate, depth of fusion, width of bead, formation of fine grains. The hardness values of the beads are higher than the base metal. The formation of the precipitates along the grain boundaries adversely increases the hardness and toughness of the beads. The dendrites and the ripple formation on the surface of the beads gradually decreases on increasing the heat input.*

***Key Words*: Alloy 617, preheat, hot wire, weld bead, ripple, etc**

1. INTRODUCTION

The gas tungsten arc welding process uses the heat produced by an arc between a nonconsumable tungsten electrode and the base metal. The molten weld metal, heated weld zone, and nonconsumable electrode are shielded from the atmosphere by an inert shielding gas that is supplied through the torch. An electric arc is produced by an electric current passing through an ionized gas. In this process, the inert gas atoms are ionized by losing electrons and leaving a positive charge. The positive gas ions then flow from the positive pole to the negative pole and the electrons flow from the negative pole to the positive pole of the arc. The intense heat developed by the arc melts the base metal and filler metal (if used) to make the weld. As the weld pool cools, coalescence occurs and the parts are joined. The occurrence of spatter or smoke is minimized. The resulting weld is smooth and uniform and requires minimum finishing. Filler metal is not added when thinner materials, edge joints, or flange joints are welded. This is known at autogenous welding. For thicker materials an external filler or "cold" filler rod is generally used. The filler metal in gas tungsten arc welding is not transferred across the arc but is melted by it.

1.1 Hot wire gas tungsten arc welding process

The process for hot wire addition is similar to the cold wire process, except that the wire is resistance heated nearly to its melting temperature at the point of contact with the weld pool. When using the preheated wire in mechanized and automatic GTAW, the wire is fed mechanically to the weld pool through a holder to which inert gas may be added to protect the hot wire from oxidation. The hot wire process increases arc energy available to melt base material, thus in addition to increasing the deposition rate, the hot wire process is usually run at higher welding speeds than cold wire systems. The hot wire process is normally used in the flat welding position because of its higher deposition rates. Out-of-position welding has been done, but with limited success. While hot wire has not been used as extensively as cold wire, the hot wire system also produces high quality weld deposits characteristic of the gas tungsten arc process. To accommodate increased deposition rates and weld pool sizes and to promote more desirable weld geometry, a mixture of shielding gases, such as 75% helium and 25% argon, is used in many applications. When welding at higher deposition rates and welding speeds, additional shielding gas can be supplied by trailing the gas shields to aid in protecting the solidifying weld metal. The deposition rate is greater with hot wire than with cold wire. This rate can approach those of gas metal arc welding when welding at high currents. The current flow in the wire is initiated when the wire contacts the weld surface. The wire is usually fed into the weld pool directly behind the arc at a 40° to 60° angle relative to the tungsten electrode. The wire is normally resistance heated by alternating current from a constant-voltage power source, although some systems apply direct current. Alternating current is used for heating the wire to avoid arc blow (deflection toward or away from the filler wire). Hot wire filler has been used successfully for cladding applications and for welding a range of steels, stainless steels, nickel and copper alloys, and reactive metal such as titanium. Hot wire additions are not recommended for aluminum and copper because the low resistance of these filler wires requires high heating current, which results in excessive arc deflection and uneven melting.

2. BASE MATERIAL

The base metal for welding is chosen as alloy 617 tube. The dimensions for tube is length 478 mm, outer diameter 52 mm, inner diameter 27 mm and wall thickness 12.mm. The distance between each bead are maintained up to 20 mm. The

ASTM standard for the Alloy 617 tube is ASTM B546 – 04(Standard Specification for Electric Fusion-Welded Ni-Cr-Co-Mo Alloy (UNS N06617).

Table -1: Chemical composition of base metal and filler metal

S. No	Element	% Present	
		Base metal	Filler metal
1	C	0.15	0.15
2	Ni	44.0	46.00
3	Fe	3.00	3.00
4	Si	0.50	1.00
5	Mn	0.50	1.00
6	Co	15.0	15.0
7	Cr	24.0	24.0
8	Ti	0.60	0.60
9	P	0.015	0.03
10	S	0.015	0.015
11	Mo	10.0	8.0
12	Al	1.50	0.80
13	B	0.006	0.006
14	Cu	0.50	0.50

2.1 Filler material

The filler wire ErNiCrCoMo-1 is selected with reference to ASME Boiler & Pressure Vessel Code (2015), Section II, Part C, SFA 5.14, Specification for Nickel and Nickel-alloy bare Welding electrodes and rods. The tungsten electrodes of ceriated type is used welding. The ceriated tungsten electrodes contains about 98% of tungsten as major element and 2% of cerium as minor element. The ceriated electrodes are known for the best performance in DC welding for welding of thin sheets and also can be used in AC process. The ignition of arc at low current makes the ceriated electrodes of tungsten as become popular for orbital tube and pipe welding, joining of thin sheets and welding of compact parts. The filler metal is selected in match to composition of the base metal.

3. PROCESS PARAMETERS

- Current (I): 100, 150 & 200 A
- Hot wire current (I_{hot}): 30, 40 & 50 A
- Filler wire diameter (mm): 1 mm
- Filler wire: ErNiCrCoMo-1
- Welding speed: 100mm/min
- Wire feed speed: 700mm/min
- Shielding gas: Argon
- Gas flow rate: 15 lpm
- Electrode diameter: 3.2 mm
- Stringer bead technique
- Angle of welding: 270°
- Welding position: 1G
- Diameter of tube: 52 mm
- Wall thickness of tube: 12.5 mm

3.1 Welding process

Hot Wire Gas Tungsten Arc (HW-GTA) welding on Alloy 617 tube was carried out using 1.0 mm diameter nickel alloy filler wire of grade ErNiCrCoMo-1 with Panasonic-YC400 direct current (DC) welding power source. During the welding process, the tube was rigidly fixed in a fully automated welding lathe that has synchronized rotation of head and tail stock. The welding power source, welding torch, mechanized hot wire feeder and automatic torch positioning system were fitted on welding lathe. The welding parameters such as welding current (I), wire feed rate (WFR), hot wire current (I_{hot}), welding speed, filler wire extension and arc gap were programmed and controlled using the control panel attached with the welding lathe. Entire operation of HW-GTAW was monitored and controlled using a M/s. W. Tech make PLC programmer. Commercial pure argon (99.98%) shielding gas was passed at 15 lpm during the welding operation.

4. CALCULATION OF COOLING RATE

The different nature of characteristic pattern of ripples on the surface of weld deposit left behind by the solidifying weld pool due to variation in heat input and total heat transferred to the weld pool under different welding parameters has been considered to estimate the cooling rate. Cooling rate prevails in solidifying weld bead. The weld bead surface characteristics such as the length of ripple lag (L_{rg})and width of molten pool (W_{rg}), have been measured by using the photographs captured in microscope. The studies have been carried out by taking at least 10 measurements on the ripples of 5–6 locations of the weld bead to ensure the true representation of the ripple characteristics, and the results are analyzed statistically. In consideration of these surface characteristics, the cooling rate (CR) of weld deposit has been estimated as follows.

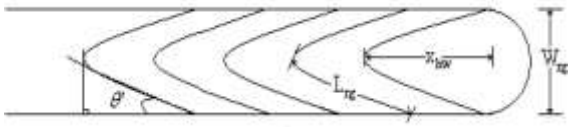

Fig -1: Weld bead profile

$CR = GR_G$

where G is solidification temperature gradient and R_G are growth rate of solid. The G and R_G has been estimated as

$G = T_m/x_{hw}$

$RG = S \times \sin \Theta$

where Tm and S are the melting temperature of base plate and welding speed, respectively, and the xhw and Θ are the distance between the heat source and rear of the weld pool and angle between the welding direction and direction of growth of solidification, respectively.

5. CALCULATION OF HEAT INPUT

The effect of HW-GTAW process variables on the heat input (HI) of hot wire GTAW process has been estimated by considering energy produced through welding arc and hot wire addition as follows.

$$HI = \frac{I^2 hot \times Rh}{Vw} + \frac{V \times I \times 0.6}{S}$$

where, I is welding current, I_{hot} is hot wire current, V is arc voltage, S is welding speed (cm/min), V_w is wire feed speed (m/min) and R_h is resistance of filler wire (Ω). R_h can be estimated by considering resistivity of filler material (ρ, Ωm), filler wire extension (L, mm) and cross-sectional area of filler wire (A_w, mm^2) as shown below.

$$R_h = \frac{\rho L}{Aw}$$

6. RESULTS AND DISCUSSION

6.1 Microstructure of base metal

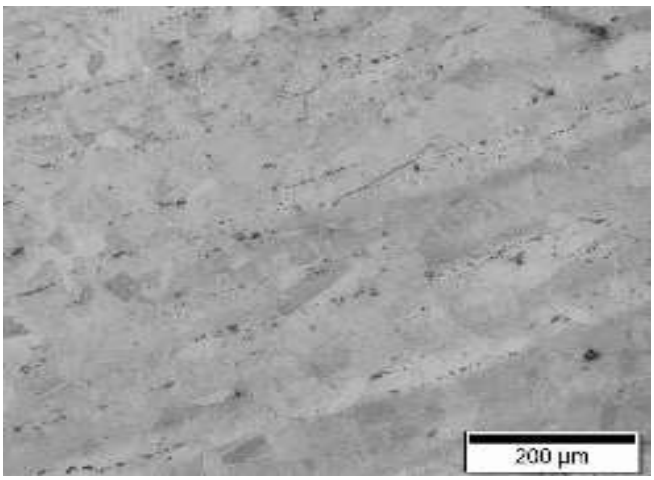

Fig -2: Microstructure of base metal (100X)

6.2 Macrostructure of weld beads

The macrostructure of the beads is taken at a magnification of 75X. The macrostructure of the beads is captured with the help of Leica stereo microscope. The macrostructure of the beads for three welding currents (100A, 150A and 200A) are shown below.

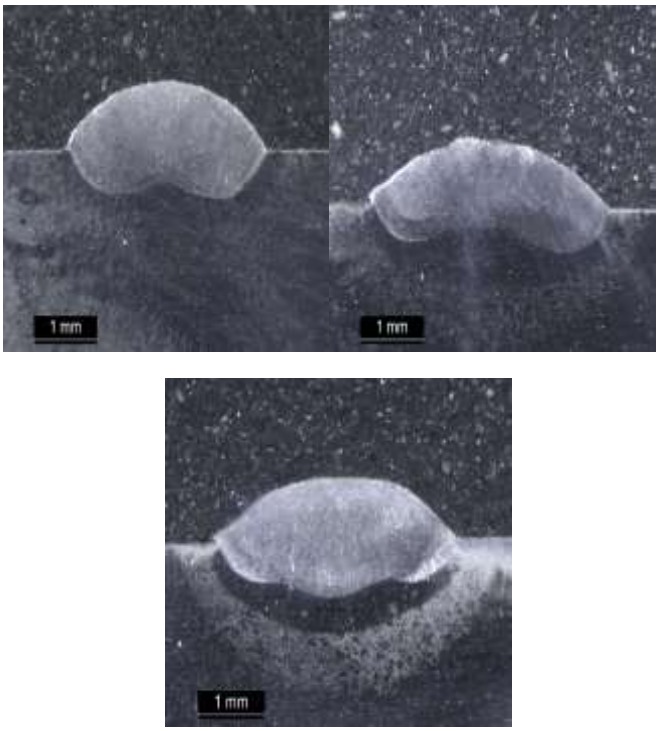

Fig -3: Macrostructure for I_{hot}= 30,40,50A. I=100A

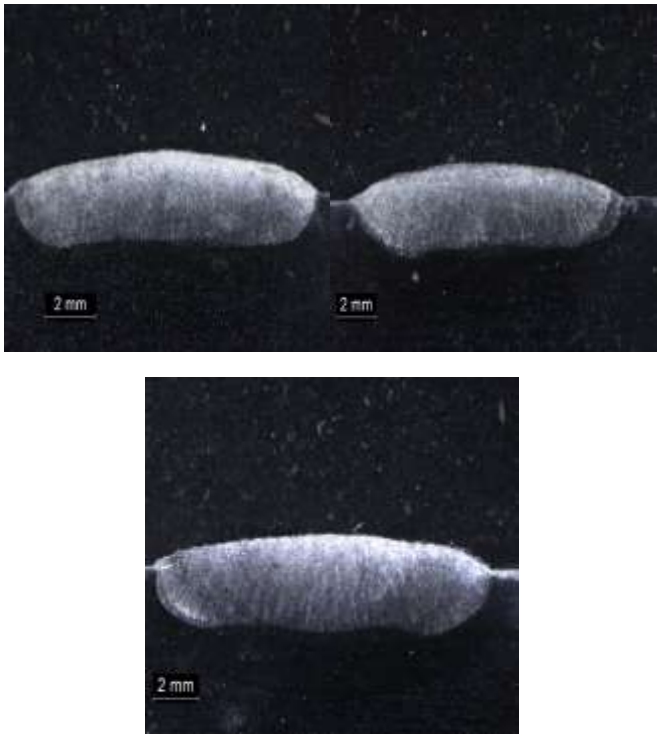

Fig -4: Macrostructure for I_{hot}= 30,40,50A. I=150A

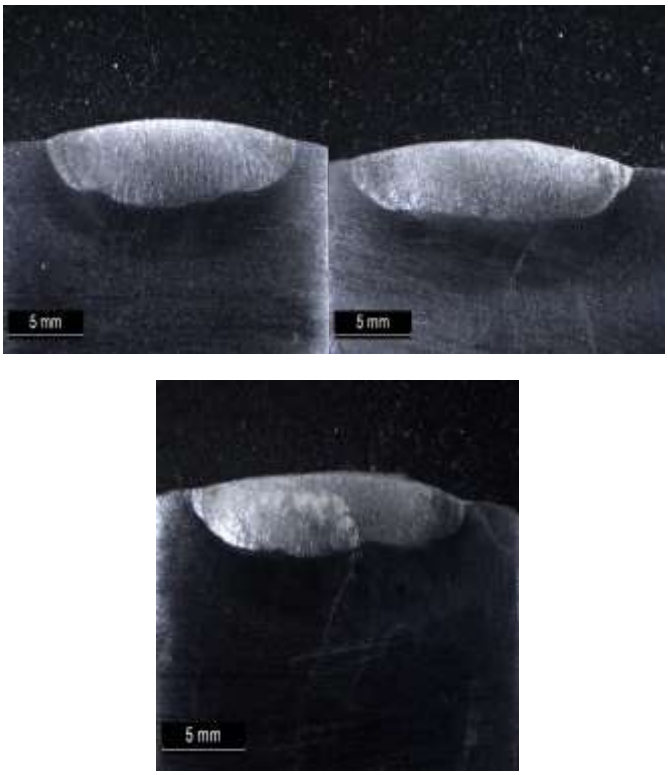

Fig -5: Macrostructure for I_{hot}= 30,40,50A. I=200A

The width of the bead increases with increasing the welding current. For increasing three hot wire currents the deposition rates increases gradually, despite of being increasing welding currents. The depth of fusion decreases with increasing the welding current. So, by increasing the welding current(I) along with hot wire current(I_{hot}), the deposition rate increases.

6.3 Microstructure of weld beads

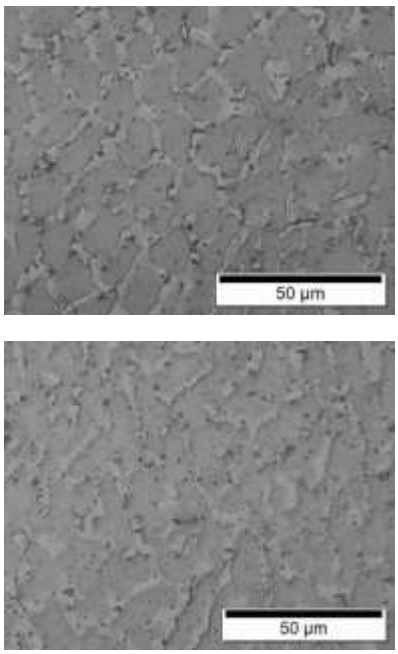

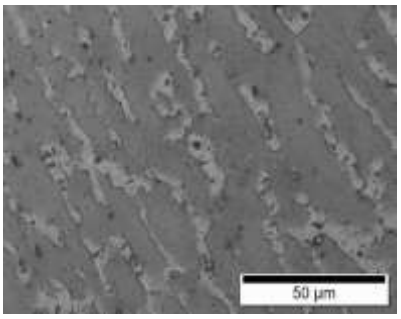

Fig -6: Microstructure for 1,2,3 beads(500X)

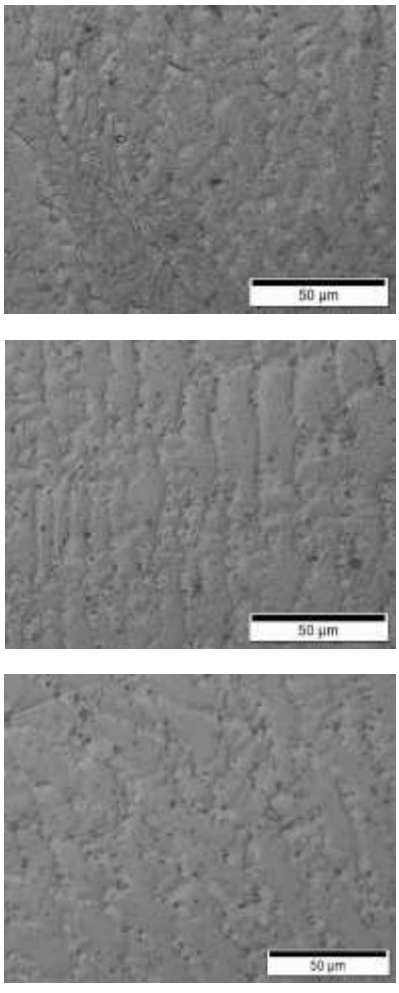

Fig.7: Microstructure for 4,5,6 beads(500X)

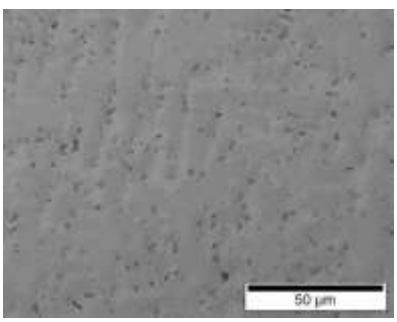

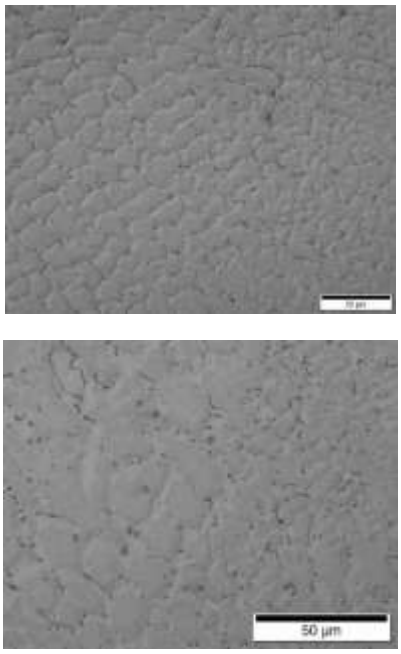

Fig.8: Microstructure for 7,8,9 beads(500X)

The microstructure of the alloy 617 base metal contains titanium, aluminium and niobium which forms as a strengthening precipitate with nickel after welding. These precipitates are coherent with the austenite matrix and thus the strength of the alloy increases substantially. The most common precipitates are called gamma prime [γ′ - Ni_3Al, Ni_3Ti, and $Ni_3(Ti, Al)$] and gamma double prime (γ″ - Ni_3Nb). The microstructure of the weld beads is shown in the tables. The microstructure is taken at three different magnification of 100X, 200X and 500X. The grain size of weld beads becomes fine grains to coarse grains on increasing the welding current along the hot wire current. The hot wire current in addition with welding current provides proper recrystallization temperature for the grains. On increasing the currents (I and I_{hot}) the strength and width of the precipitation grain boundary gets gradually denser causing the coherent austenite phases stronger to high temperature strength, toughness, and resistance to degradation in corrosive or oxidizing environments.

6.3 Vickers microhardness survey

The specimens were cut to a size of 20 x 12.5 x 9 mm for hardness testing and were polished using standard metallographic procedure. The magnification for the microhardness survey was fixed at 400X. The force used for microhardness survey is 300gf. The dwell time is maintained at 25.5 seconds. Micro hardness surveys were made on these specimens using Vickers hardness test along the direction of thickness from top surface of bead to the base metal in transverse direction of thickness after every 300 µm for first three beads and 200 µm for next six beads. The hardness values are plotted in the form of a graph. The result indicate that the hardness values are more on the bead area and decrease towards the fusion boundary region and remain constant on the base metal for all the nine beads.

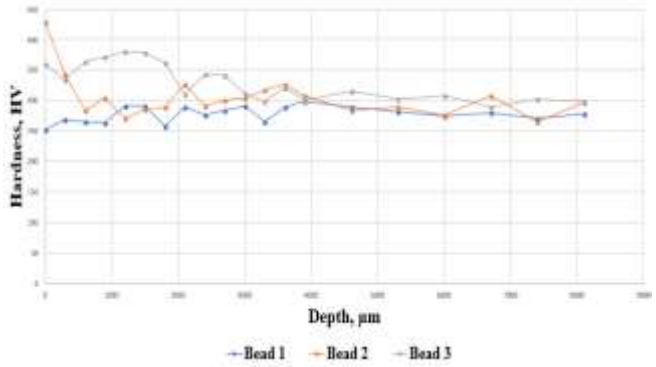

Chart -1: Hardness Value for beads 1,2,3

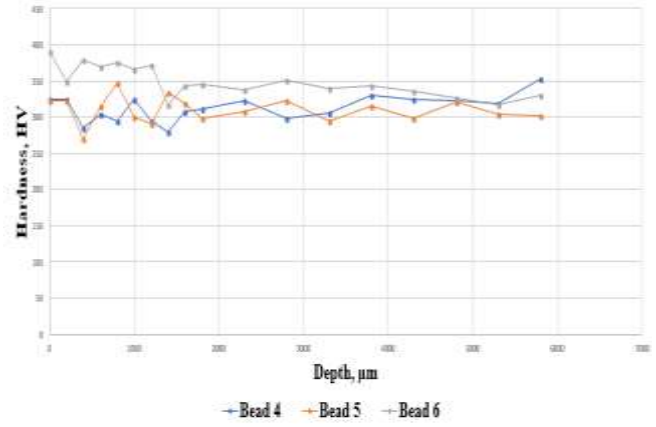

Chart -2: Hardness Value for beads 4,5,6

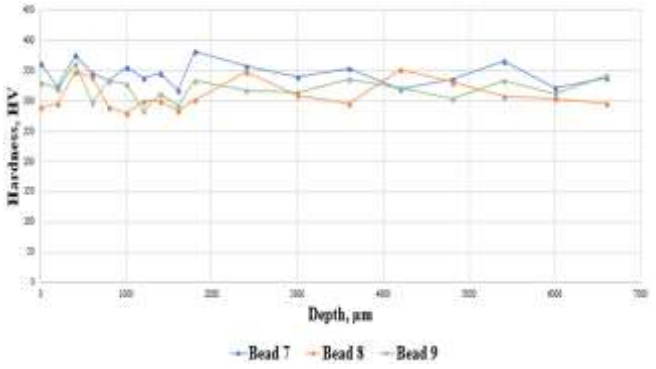

Chart -3: Hardness Value for beads 7,8,9

6.4 Calculation of cooling rate

The cooling rate is calculated with the help of measuring the dimensions of the length of ripple lag(L_{rg}), distance between the heat source and rear of the weld pool(x_{hw}), width of molten pool(W_{rg}) and angle between the welding direction and direction of growth of solidification (Θ) with the help of microscope. The readings are taken by measuring the parameters. The readings are tabulated and the cooling rates are calculated. The cooling rate is controlled by the heat input, by the temperature at which welding starts and by the thickness of the tube being welded. Fast cooling rate leads to a finer microstructure, usually to a less coarse

microstructure, higher hardness and greater strength. The cooling rate for the nine beads shows that it decreases with increase in welding current. Higher heat input for higher currents makes the rate of cooling slower.

Table -2: Cooling rates for the nine beads

Bead No.	1	2	3	4	5
Cooling rate ºC/sec	662.6	640.7	631.0	516.4	488.5
Bead No.	6	7	8	9	
Cooling rate ºC/sec	465.01	422.03	409.42	403.17	

3. CONCLUSIONS

The macrostructure of the beads reveals that the width of the bead increases with increasing the welding current. The depth of fusion decreases with increasing the welding current. So, by increasing the welding current(I) along with hot wire current(I_{hot}), the deposition rate increases. The microstructure of the alloy 617 base metal contains titanium, aluminium and niobium which forms as a strengthening precipitate. These precipitates are coherent with the austenite matrix and thus the strength of the alloy increases substantially. The grain size of weld beads becomes fine grains to coarse grains on increasing the welding current along the hot wire current. Micro hardness survey results indicate that the hardness values of beads are greater than base metal and decrease towards the fusion boundary region and remain constant on the base metal for all the nine beads.

The calculation of cooling rate shows that fast cooling rate leads to a finer microstructure, higher hardness and greater strength. The cooling rate for the nine beads shows that it decreases with increase in welding current. Higher heat input for higher currents makes the rate of cooling slower.

REFERENCES

[1] Anantha Padmanabhan MR., Baskar Neelakandan and Devakumaran Kandasamy (2016) 'A study on process characteristics and performance of hot wire gas tungsten arc welding process for high temperature materials', Materials Research, Vol 20, No.4, pp 76-87.

[2] David S.A. and Vitek J.M. (1989) 'Correlation between solidification parameters and weld microstructures', International Materials Reviews, Vol 34, No.5, pp 213-245.

[3] Devakumaran K. and Ghosh P.K. (2010) 'Thermal Characteristics of Weld and HAZ during Pulse Current Gas Metal Arc Weld Bead Deposition on HSLA Steel Plate', Materials and Manufacturing Processes, Vol 25, No.7, pp 616-630.

[4] Hyun Cho, Kwang Hyun Bang and Byeong Woo Lee (2010) 'Influence of refractory ceramic coatings on high temperature properties of Inconel 617', Surface & Coatings Technology, Vol 205, pp 409-413.

[5] Pavan A.H.V., Vikrant K.S.N., Ravibharath R. and KulvirSingh (2015) 'Development and evaluation of SUS304H — IN 617 welds for advanced ultra-super critical boiler applications', Materials Science and Engineering, Vol A 642, pp 32–41.

[6] Poorhaydari K., Patchett B.M, and Ivey D.G. (2005) 'Estimation of Cooling Rate in the Welding of Plates with Intermediate Thickness', Welding Journal, Vol 5, pp 149-155.

[7] Rahul Kumar, Harish K Arya and Saxena RK. (2014) 'Experimental Determination of Cooling Rate and its Effect on Microhardness in Submerged Arc Welding of Mild Steel Plate', Journal of Material Sciences & Engineering, Vol 3, No.2, pp 360-363.

[8] Rahman S., Priyadarshan G., Raja K.S., Nesbitt C. and Mishra M. (2008) 'Investigation of the secondary phases of Alloy 617 by Scanning Kelvin Probe Force Microscope', Materials Letters, Vol 62, pp 2263–2266.

[9] Shah Hosseini H., Shamanian M. and Kermanpur A. (2016) 'Microstructural and weldability analysis of Inconel617/AISI 310 stainless steel dissimilar welds', International Journal of Pressure Vessels and Piping, Vol 144, pp 18-24.

[10] Shah Hosseini H., Shamanian M. and Kermanpur A. (2011) 'Characterization of microstructures and mechanical properties of Inconel 617/310 stainless steel dissimilar welds', Materials Characterization, Vol 62, pp 425-431.

[11] Wenjie Ren, Fenggui Lu, Pulin Nie, Renjie Yang, Xia Liu, Kai Feng and Zhuguo Li (2017) 'Effects of the long-time thermal exposure on the microstructure and mechanical properties of laser weldings of Inconel 617', Journal of Materials Processing Technology, Vol 17, No.3, pp 171-188.